# ON THE EFFECT OF CALCIUM LIGNOSULFONATE ON THE RHEOLOGY AND SETTING TIME OF CEMENT PASTE

**A. Colombo (1), M. R. Geiker (1), H. Justnes (2,3), R. A. Lauten (4), K. De Weerdt (1)**

(1) Department of Structural Engineering, Norwegian University of Science and Technology, Trondheim, Norway

(2) SINTEF Building and Infrastructure, Trondheim, Norway

(3) Department of Materials Science and Engineering, Norwegian University of Science and Technology, Trondheim, Norway

(4) Borregaard, Sarpsborg, Norway

## ABSTRACT

The effect of softwood calcium lignosulfonate, LSs, on the rheology and setting time of cement paste has been investigated. Two Portland cements with different surface area and $C_3A$ content were used. The lignosulfonate was added either immediately with the mixing water or delayed after 10 minutes of hydration. The cement pastes were characterized in terms of specific surface, rheology and heat of hydration. Extracted pore solutions were analysed for free lignosulfonate concentration and for changes in elemental composition. Immediate addition of LSs increased the specific surface, but not delayed addition. Correlations were found between rheology and surface coverage by LSs, as determined by adsorption isotherms, and between the setting time and the amount of free LSs in the pore solution. An increased setting retardation upon delayed addition related to an increased concentration of Al in the pore solution.

**KEYWORDS**

Lignosulfonate; admixture; rheology; setting retardation; adsorption

# 1 INTRODUCTION

Water-reducers, or plasticizers, are commonly used admixtures for concrete. Their addition to fresh concrete allows obtaining highly fluid concrete at low water-binder ratios, improving the mechanical properties and the durability of the hardened concrete [1, 2]. The plasticizer used in this paper is a low-sugar softwood calcium lignosulfonate (LSs), commonly used in concrete in dosages 0.25-0.40 mass % of binder. Lignosulfonates are polyelectrolytes derived from lignins in the pulping industry. Lignin can be derived from various sources of biomass, and lignosulfonates of different molecular weight and amount of functional groups (carboxyl groups, phenolic-OH, sulfonic groups) can be produced.

The dispersing effectiveness of plasticizers on cementitious materials is, amongst others, a function of the degree of adsorption on the surface of the cement grains and hydrates. There are two main dispersing mechanisms: electrostatic repulsion and steric hindrance. Which of the mechanisms is dominant depends on the plasticizer type. During electrostatic repulsion the adsorbed plasticizer layer renders the particle surface negatively charged, i.e. with a negative zeta potential. As negatively charged particles approach each other, electrostatic repulsion prevents them from forming agglomerates. Additionally, when two surfaces approach close enough for their adsorbed layers to overlap, a steric force develops. This will contribute in hindering particles to get close enough to form agglomerates. The key parameters that govern the steric repulsion are the adsorption layer thickness and its conformation at the solid liquid interface [3]. Lignosulfonate can disperse cement particles by both electrostatic repulsion and steric hindrance, as reported by Vikan [4], amongst others.

In addition to dispersion, the interaction between cement and plasticizer can potentially lead to retardation of the setting time of the cement paste. Several mechanisms of retardation are hypothesized in the literature, the main ones being: calcium complexation, nucleation poisoning of hydrates, surface adsorption on anhydrous cement particles, and presence of sugars in the plasticizer [5-8]. Calcium complexation involves the interaction between plasticizing polymers and calcium ions in the pore solution. This would slow down the build-up of calcium supersaturation needed for hydrates nucleation. However, according to Bishop et al. [5], and Marchon and Flatt [7], amongst others, the

low dosages of plasticizers generally used limit the amount of calcium potentially complexed. Thus, calcium complexation does not appear likely as a main mechanism of setting retardation of cement. As stated by Thomas and Birchall [9] and Marchon and Flatt [7] amongst others, retardation by nucleation poisoning of hydrates is where the plasticizer poisons the nuclei of CH, preventing its growth. By suppressing CH precipitation, $C_3S$ dissolution is delayed, as the degree of calcium saturation in the pore solution is unaltered. Hence, C-S-H precipitation is hindered, which leads to prolongation of the induction period of the cement paste [7]. Surface adsorption of the plasticizer on unhydrated cement grains might reduce the dissolution of the clinker phases and cause retardation. This, in turn, retards the formation of hydrates, prolonging the induction period of the cement paste [7]. Finally, the sugars contained in the plasticizers generally delay the onset of the acceleration period, by adsorbing on anhydrous phases like $C_3S$, but also on cement hydrates, especially CH [10]. In conclusion, the mechanisms that most likely retard the cement setting appear to be related to (1) the plasticizers poisoning the nuclei of CH, retarding $C_3S$ dissolution and C-S-H precipitation, (2) the reduced dissolution of clinker phases, and (3) the possible presence of sugars in the plasticizer.

Lignosulfonates are known to have a retarding effect on cement hydration [11-13]. The sugars naturally contained in lignin contribute to longer setting times of cement, in particular the hexoses. The sugars can be almost completely removed, however also sugar-reduced LS can cause retardation [14]. Several studies concluded that the addition of calcium lignosulfonate changes the hydration of $C_3S$ and $C_3A$ [13, 15-19]. According to Ramachandran [18], a strongly surface-bound calcium lignosulfonate complex could be detected for both $C_3A$ and $C_3S$, which could cause retardation of $C_3A$ and $C_3S$ hydration. In another paper [15], Ramachandran stated that the retardation effect of calcium lignosulfonate depends on its concentration in solution and not on its proportion with respect to $C_3S$. $C_3S$ hydration was delayed in proportion to the concentration, and it practically stopped for concentrations above 3 g/l of water. On the contrary, $C_3S$ hydration was found to speed up for lignosulfonate concentrations under 1 g/l of water. Monosi et al. [16] found that, in a $C_3A$-$C_3S$ system, the addition of calcium lignosulfonate led to a strong retardation in $C_3S$ hydration, while $C_3A$ hydration was slightly accelerated. The retardation in the $C_3A$-$C_3S$ system was lower than that in pure

$C_3S$ systems. In fact, the lignosulfonate adsorption by $C_3A$ decreases the concentration of polymer available to retard the $C_3S$ hydration. Moreover, the arrest in $C_3S$ hydration is partially counterbalanced by the increase in rate of hydration of $C_3A$, as stated by Collepardi et al. [17]. In conclusion, lignosulfonate was found to retard $C_3S$ hydration [13, 18] depending on its concentration in the pore solution [15]. $C_3A$ hydration was found to be retarded by lignosulfonate by some authors [13, 18, 19], while not retarded [20] or slightly accelerated [16, 17] by other authors.

As described by e.g. Flatt and Houst [21], the addition time of the plasticizer to the cement paste greatly affects the amount of plasticizer consumed by the cement paste and the extent of retardation. It has to be noted that the influence of the addition time was found to be lower for admixtures like polycarboxylic superplasticizers [22, 23]. Several studies, amongst others Uchikawa et al. [24], Chiocchio and Paolini [25], Aiad et al. [26], found that, at equal plasticizer dosage, the flow of cement paste prepared by delayed addition is higher than that of cement paste prepared by immediate addition. Moreover, the setting is further retarded in case of DA. Chiocchio and Paolini [25] found that the optimum addition time of plasticizer to achieve the maximum workability corresponds to the beginning of the dormant period of the cement hydration without admixture. Hot [27], Hsu et al. [28], and Aiad [29] found that the optimum addition time was between 10 and 15 minutes after water addition.

The rheological behavior of fresh cementitious materials is generally characterized by yield stress ($\tau$) and viscosity ($\mu$). As described by e.g. Roussel et al., the yield stress corresponds to the energy needed to break down a network of interaction between particles in a cementitious system. Its origin lays in colloidal and contact interactions between particles. Viscosity results from hydrodynamic, colloidal and contact forces involved in the motion of the suspended cement grains. The yield stress is often considered as the most relevant parameter to describe workability and the ability of a material to properly fill a mold under its own weight. However, the viscosity also seems to be a very relevant parameter to describe cement or concrete workability, especially for systems with low water-binder ratio [30, 31]. Plasticizing admixtures can change both yield stress and viscosity by adsorbing on cement particles and changing the flocculation state of cement paste [31].

106 The subject of this paper is to investigate the effect of LSs on the rheological properties and setting
107 time of two Portland cements with different physical and chemical properties (e.g. surface area, $C_3A$
108 content). The samples were studied both by adding the lignosulfonate immediately with the mixing
109 water (IA) and by adding it after 10 minutes hydration (DA). The results were compared to the
110 adsorption isotherms presented in a previous paper by the same authors [32]. The amount of polymer
111 consumed by the cement paste was related to the changes in rheological properties and hydration
112 kinetics of the cement pastes due to LSs addition. Changes in the surface area of the hydrated cement
113 particles were investigated by BET. The elemental composition of the pore solution extracted from the
114 cement paste samples was analysed with ICP-MS. The results of this paper will contribute to a deeper
115 understanding on the physical and chemical mechanisms behind the changes in rheological properties
116 and setting time of cement paste with lignosulfonate.

117 # 2 EXPERIMENTAL
118

119 ## 2.1 Materials

120

121 The experiments were performed on two different cements: a CEM I 52.5 N (ANL) and a CEM I 52.5
122 R (CX), as defined in the European standard EN197-1. The content of the main clinker phases of the
123 cements quantified by XRD Rietveld, according to the technique described in [33], are given in Table
124 1. The chemical composition of the cements determined by XRF and the loss of ignition at 950 ºC are
125 reported in Table 2. The particle size distribution ($d_{10}$, $d_{50}$, $d_{90}$), Blaine and BET surface area, and
126 density are given in Table 3.

127 A sugar-reduced softwood calcium lignosulfonate (LSs) was used as plasticizer. Its mass weighted
128 molecular weight ($M_w$), as measured with gel permeation chromatography (GPC), was 29000 g/mol
129 and the number weighted molecular weight ($M_n$) was 2100 g/mol, giving broad molar-mass dispersity
130 ($Đ_M$) equal to 13.8. The molar-mass dispersity, also called polydispersity index, is defined as the ratio
131 between $M_w$ and $M_n$ [34]. Additional physical and chemical properties of the lignosulfonate are listed
132 in Table 4. For the lignosulfonate used in the present investigation, the sugars were removed from the

polymer molecule by fermentation and resulting alcohol by distillation. The LSs was dissolved in deionised water to concentrations varying from 1 to 45 % to ease dosing, and the water content was included in the calculation of the water-to-binder ratio (w/b).

## 2.2 Sample preparation

About 300 g cement was mixed with deionised water and/or lignosulfonate solution in a high-shear MR530 by Braun mixer at intensity 6 obtaining a paste with w/b = 0.4. A cement paste volume of about 200 ml was mixed for all the cement pastes. In order to investigate the effect of the time of addition of lignosulfonate, two different mixing procedures were applied: immediate addition of LSs with the mixing water (IA) and delayed addition of LSs after 10 minutes of hydration (DA).

For IA, the binder was mixed with deionised water (and/or lignosulfonate diluted in deionised water) according to the procedure used by Vikan : 30 seconds mixing, scraping the mixer walls to homogenize the mix, 5 minutes resting and 1 minute mixing.

For DA, the binder and 85% of the water were mixed according to the following mixing procedure: 30 seconds mixing, scraping the mixer walls to homogenize the mix, 10 minutes resting (delay time chosen according to several studies in literature [25, 27-29]). LSs diluted in the remaining 15% of the needed water were then added to the mix, which was mixed for 1 minute.

## 2.3 Methods

### 2.3.1 Rheological measurements

The rheological properties were measured with a Physica MCR 300 rheometer using parallel plates with serrated surfaces of 150 μm depth. The radius of the plates was 30 mm and the gap between the plates was set to 1 mm. The bottom plate or stator was kept at a constant temperature of 20 ºC. Some drops of deionized water were put in the water trap located on the upper plate or rotor and an enclosure was used to limit evaporation of water from the paste sample during the measurement.

After the mixing sequence (as described in paragraph 2.2), about 2.5 ml of cement paste was placed on the bottom plate of the rheometer, and the rheological measurement was started 10 minutes after water addition. Up-down flow curves were measured at 10, 20 and 30 minutes of hydration. For the samples to which the plasticizer was added at 10 minutes hydration (DA), the first flow curve was measured at 12 minutes of hydration instead of 10 minutes. Before every measuring cycle, the paste was stirred for 30 seconds at the constant shear rate of 60 $s^{-1}$. The measuring sequence, described in Table 5, allowed measuring the shear stress of cement paste as the shear rate increased from 0 to 60 $s^{-1}$ (up flow curve) or decreased from 60 to 0 $s^{-1}$ (down flow curve).

The flow curves generally showed a pronounced shear-thinning behavior. The Bingham model was applied to the second part of the down flow curve, obtained for shear rate between 26 and 60 $s^{-1}$. The linear fitting of this flow-curve segment allowed the calculation of the dynamic yield stress, $\tau_0$, as the extrapolated intercept with the ordinate, and of the plastic viscosity, $\mu_p$, as the slope of the linear fit.

In addition, the results from the rheological measurements are also presented in terms of flow resistance, as defined by Vikan et al. in [35]. This value is calculated as the area under the entire flow curve (shear rate from 1 to 60 $s^{-1}$), and it represents the power necessary to make a certain volume of sample flow at a chosen shear rate range ($W/m^3$ or Pa/s).

### 2.3.1 Isothermal calorimetry

Isothermal calorimetry was carried out at 20˚C in a TAM Air eight-channel isothermal calorimeter produced by Thermometric AB. The evolution in time of the heat of hydration of ANL and CX cements was measured for different dosages of LSs and both for IA and DA of plasticizer. The samples were prepared as described in paragraph 2.2. After mixing, about 6 g cement paste was placed in a 20 ml glass ampoule, which was sealed and placed in the calorimeter. The heat of hydration was recorded for 60 hours.

### 2.3.2 UV-spectroscopy

UV-spectroscopy allowed measuring the LSs concentration in the extracted pore solution from the cement paste samples.

After mixing according to section 2.2, about 35 ml paste was poured in 50 ml plastic centrifuge tubes and let to rest until the chosen analysis time. The pore solution was extracted from the cement paste by centrifuging the samples in a Heraeus Megafuge 8 centrifuge by Thermo Scientific for 3 minutes at the speed of 4500 rpm. The supernatant pore solution was extracted and filtered with 0.45 µm syringe filters. The pore solution was analysed with a Genesys 10S UV-spectrophotometer by Thermo Scientific. Wavelengths in the range 280-284 nm had been reported in literature to study the adsorption of lignosulfonate on cement particles [3, 4, 24, 36, 37]. When scanning the absorbance of an LSs solution for the wavelengths in the range of 190 to 350 nm, a clear absorbance peak was observed with a maximum at approximately 281 nm. The maximum intensity of the absorbance peak at 281 nm increased linearly with increasing LSs dosage. The absorbance at this wavelength, 281 nm, was therefore used to determine the LSs concentration in solution.

With the help of a calibration curve, obtained measuring the absorbance of solutions of different concentrations of LSs in deionised water, the amount of free plasticizer (g LS/100 g solution) could be determined. This amount was related to the amount of binder in the sample (g LS/100 g binder). The LSs consumed by the investigated systems was then calculated by subtracting the amount of free LSs from the total amount of LSs added to the sample, as displayed in equation 1:

$$LSs_{consumed} = LSs_{total} - LSs_{free} \quad (1)$$

Polymer adsorption by a solid is usually described using isotherms, in which the amount of polymer adsorbed is plotted against the total amount of polymer added to the system [38]. The shape of an isotherm is largely determined by the adsorption mechanism. In this study, the isotherms were drawn relating the amount of LSs consumed by the cement paste to the amount of total LSs added to the sample.

Initially, the free plasticizer in the pore solution extracted from the cement paste was measured by UV-spectroscopy at increasing hydration time (from 5 to 120 minutes hydration). It was found that at 10

minutes hydration the LSs uptake reached an equilibrium value. All the samples were then analysed at 30 minutes hydration.

### 2.3.3 Solvent exchange

A solvent exchange procedure with isopropanol was used to stop the hydration of the cement paste after 30 minutes of hydration.

About 5 ml of cement paste was transferred in a 50 ml centrifuge tube and centrifuged for 1 minute at 2000 rpm. The supernatant was removed. About 40 ml of isopropanol was poured in the centrifuge tube. The tube was shaken for 30 seconds and let to rest for 5 minutes. The sample was centrifuged again for 1 minute at 2000 rpm and the supernatant liquid was removed. The solvent exchange procedure with isopropanol was repeated once, followed by a final solvent exchange with 10 ml of petroleum ether. The resulting paste was let to dry for 2 days in a desiccator over silica gel, and soda lime to minimize carbonation. After drying, the samples were ground to powder and homogenized in a porcelain mortar and stored in sealed containers in a desiccator over silica gel and soda lime until analysis.

### 2.3.4 BET of hydrated cement pastes

The BET measurements were performed using a Tristar II Plus by Micromeritics on cement paste samples of which the hydration was stopped with the solvent exchange procedure. The measurements were performed purging the samples with nitrogen. The samples were degassed in vacuum before the measurement, and the measurement was performed at 20 ºC.

### 2.3.5 ICP-MS of pore solution

ICP–MS (inductively-coupled plasma mass spectrometry) was used to determine the elemental concentration of Al, Ca, Fe, K, Na, S and Si in the pore solution extracted from the cement paste. The

pore solution was extracted from ANL and CX cement pastes with 0, 0.8, 1.5 mass % LSs mixed both with IA and DA. The solution was filtered with the same procedure used for UV-spectroscopy (paragraph 2.3.2) and acidified prior to analysis by adding 1:1 by volume of 1:10 diluted $HNO_3$.

# 3 RESULTS

## 3.1 Rheological properties

The rheology of ANL and CX cement pastes was measured at 10 (12), 20 and 30 minutes of hydration with increasing dosages of LSs (0/0.4/0.8/1.5 mass % binder LSs for IA and 0/0.1/0.2/0.4 mass % binder for DA). The results at 10 (12 for DA) and 30 minutes hydration are shown in Figure 1 and in Figure 2, respectively, displaying the variation of normalized yield stress and plastic viscosity as the dosage of LSs increases, both for IA and DA. The normalized yield stress was obtained by dividing the yield stress of samples with increasing LSs dosage by the yield stress of the reference sample without LSs. The normalized viscosity was calculated according to the same principle. Table 7 gives the dynamic yield stress and plastic viscosity of the reference samples without LSs.

Increasing LSs dosage reduced both the yield stress and the viscosity of both cements both at 10 and 30 minutes of hydration, except for CX cement for IA after 30 minutes of hydration. The reduction was achieved for considerably lower LSs dosages for DA compared to IA. Less than one third LSs dosage was needed to reach the same drop in yield stress and viscosity for DA compared to IA. Regarding CX cement, a nearly constant yield stress and a remarkable increase in viscosity were measured for IA after 30 minutes of hydration with increasing LSs dosages.

Generally, a drop in yield stress would indicate LSs saturation in the cementitious system. In this study, a clear drop in yield stress was detected for DA for a LSs dosage between 0.10 and 0.25 mass % for ANL cement, and between 0.25 and 0.50 mass % for CX cement. No clear drop in yield stress was measured for IA. After 10 minutes of hydration, the yield stress decreased gradually for both cements. After 30 minutes of hydration, the yield stress showed a gradual decrease for ANL cement, while it remained nearly constant for CX cement.

The results expressed in terms of flow resistance are shown in Figure 3. The smaller the flow resistance, the less power is required to make the sample flow. The results presented in Figure 3 seem to agree with the ones presented in Figure 1 and in Figure 2, considering that slightly different regions of the flow curves were used to calculate the parameters.

Surprisingly, the yield stress of CX cement with 0.25 mass % LSs mixed with DA was higher than in the sample without LSs. However, with the same LSs dosage, the viscosity was found to decrease, and all the other conditions in the cement paste system were similar. The reason for the increase in yield stress upon 0.25 mass % DA of LSs for CX is currently not known. To understand the underlying mechanism further research is required.

### 3.2 Setting time

The effect of the LSs dosage and of its addition time on the rate of hydration and setting time of ANL and CX cement pastes can be observed in the calorimetric curves in Figure 4 for IA, and in Figure 5 for DA. Based on the definition given by the ASTM standard C1679-14 , the setting time was identified as the time to reach half of the average maximum power of the main hydration peak in the calorimetric curve. The silicates and aluminates peaks are marked with different symbols in corresponding grey shade of the respective calorimetric curve.

In the reference samples without LSs, after the initial peak of hydration, which takes place almost immediately after the contact of cement with water, two peaks could be observed: first, the peak corresponding to hydration reaction of the silicate phases (mainly $C_3S$), followed by a peak related to sulfate depletion and hydration reactions of the aluminate phases. Both the silicates and the aluminates peak were delayed by LSs addition in both cement pastes both when mixed with IA and with DA. In general, increasing LSs dosages caused a larger retardation of the silicates peak compared to the aluminates one. The two peaks even merged in most samples with the higher LSs dosages analyzed.

Moreover, for the same LSs dosage, DA resulted in a larger retardation of both peaks compared to IA. CX cement paste showed a lower retardation than ANL cement paste both for IA and DA. The

doubling of the LSs dosage led to a setting retardation between 1.5 and 2.5 times higher for CX cement, and between 4 and 5 times higher for ANL cement.

### 3.3 Concentration of aluminum ions in the pore solution

The elemental concentration of Al, Ca, Fe, Si and S in the pore solution extracted from ANL and CX cement pastes after 30 minutes of hydration was determined with ICP-MS. The LSs dosages tested were 0.8 and 1.5 mass % LSs both for IA and DA. Additionally, a reference sample without LSs was measured. Moreover, the content in Al, Ca, Fe, Si and S was also measured for two LSs solutions in artificial pore solution. The two solutions, containing 2.0 and 3.7 mass % LSs, were the ones used in the cement samples with 0.8 and 1.5 mass % LSs, respectively. The artificial pore solution was a solution of NaOH and KOH with K/Na molar ratio equal to 2 and measured pH of 12.9. The results from ICP-MS are shown in Figure 6 and reported in Table 8.

The samples mixed with DA showed an increase in Al, Fe and Si concentration in the pore solution as the LSs dosage increased. The increase was considerably larger for ANL cement than for CX cement. On the contrary, only a minor increase was measured for the samples mixed with IA.

### 3.4 Adsorption isotherms

The adsorption isotherms obtained for ANL and CX cement pastes were achieved by plotting the amount of consumed LSs after 30 minutes of hydration versus the total amount of LSs added. The tested dosages are given in Table 6. For CX cement it was not possible to extract pore solution at LSs dosages over 1.0 mass % due to paste hardening after 30 minutes hydration. The LSs was added to the cement paste either immediately together with the mixing water (IA), or after 10 minutes hydration (DA). The results per mass % binder and their fitting according to the Langmuir model [38] are presented in Figure 7.

Figure 7 shows that the cement pastes displayed similar LSs consumption at low LSs dosage (up to about 0.25 mass % LSs) independent of the time of LSs addition. At higher dosage, the curves obtained for IA differ from those obtained for DA.

For IA, no adsorption plateau could be detected within the tested range, neither for ANL nor for CX cement. The isotherms' shape indicated an increasing LSs consumption as more LSs was added to the mix.

For DA, an adsorption plateau was found for both cements. The DA isotherms displayed a considerably lower amount of LSs consumed by the cement pastes compared to the IA isotherms. The adsorption plateau was reached for a total LSs amount between 0.8 and 1.2 mass % for ANL cement, and between 1.2 and 1.5 mass % for CX cement. The authors assume the plateau to be due to the achievement of full monolayer surface coverage [32].

### 3.5 BET of hydrated cement pastes

The BET surface area was measured on ANL and CX cement pastes with varying LSs amounts after 30 minutes of hydration. The hydration was stopped by solvent exchange, as described in paragraph 2.3.3. The results are shown in Figure 8.

For both cements the surface area was found to increase as the dosage of plasticizer added to the cement paste increased. The increase in surface area was remarkably larger for IA compared to DA, and, for IA, for CX cement compared to ANL cement.

## 4 DISCUSSION

### 4.1 LSs consumption and changes in surface area

The adsorption isotherms shown in Figure 7 display a higher LSs consumption for IA than for DA.

In a previous article [32], the authors investigated the interactions between LSs and two Portland cements (the same as those used in the present paper). It was found that the LSs consumption mechanisms were different for the two cements used and for the two addition methods.

For DA, both cements' adsorption isotherms showed a plateau. According to the theory reported in [38], the achievement of a plateau in an adsorption isotherm corresponds to saturation of the available

surface for adsorption. Therefore, the LSs consumption was considered to be mainly due to monolayer surface adsorption on the surface of cement particles and hydrates.

For IA, an increase in LSs dosage was found to cause additional ettringite formation and consequently an increase in surface area of both cements after 30 minutes of hydration, to a larger extent for CX cement compared to ANL cement. This was not observed when the cements were mixed with DA [32].

A possible explanation of the difference between IA and DA is that when LS is added in the mixing water the dissolution of $C_3A$ is enhanced leading to the formation of additional ettringite. Whereas when no LSs is present in the mixing water the $C_3A$ reaction is limited, potentially by a protective hydrate layer. The delayed addition of LSs is not able to disrupt this potential protective layer initially formed, hence no additional ettringite is observed for DA.

The two cements displayed different LSs consumption mechanisms for IA. For CX cement, a large increase in ettringite formation and surface area (see Figure 8) led to a high LSs consumption [32]. No surface saturation plateau was reached, which was explained by the continuous increase in surface available for adsorption for the LSs dosages investigated. Monolayer surface adsorption on the surface of cement particles and hydrates was identified as the dominating LSs consumption mechanism for CX cement [32]. For ANL cement, the adsorption isotherm also showed a high LSs consumption without reaching an adsorption plateau. Since the amount of formed ettringite and the surface area increased only moderately compared to CX cement (see Figure 8), other polymer consumption mechanisms might have played a role for ANL cement in addition to surface adsorption.

Finally, in the same paper [32], no AFm could be detected by TGA for the investigated materials. Therefore, intercalation in AFm, as proposed, amongst others, by Flatt and Houst [21], does not appear as a feasible LSs consumption mechanism for the investigated materials and dosages.

## 4.2 Rheological properties

The obtained rheological results indicate that the addition of lignosulfonate generally improved the workability of cement paste after 10, 20 and 30 minutes of hydration, decreasing both the yield stress and the viscosity. As an exception to this general trend, after 30 minutes of hydration, CX cement mixed with IA did not show changes in the yield stress with increasing LSs dosage, while its viscosity increased about 50 %. In general, the improvement in workability was remarkably larger when the samples were mixed with DA compared to IA.

When evaluating the rheological results in light of the adsorption isotherms shown in Figure 7, it appears that a clear drop in yield stress was observed solely for the samples which reached an adsorption plateau. The samples that did not reach an adsorption plateau showed a more gradual decrease in yield stress, as for ANL cement, or no decrease at all, as for CX cement. A correlation between the achievement of surface coverage and a drop in yield stress seems to exist. Indeed, as shown in Figure 7, the isotherms obtained for DA started differing from those obtained for IA, and showing the tendency to reach an adsorption plateau, for LSs dosages over about 0.25 mass %. As shown in Figure 1 and in Figure 2, for DA, a drop in yield stress was measured for LSs dosages between 0.10 and 0.25 mass % LSs for ANL cement, and between 0.25 and 0.40 mass % LSs for CX cement. Thus, the rheological behavior seems to relate to the degree of LSs coverage of the available surface.

As shown in [32, 39], the TGA measurements performed on ANL and CX cements displayed that 1.5 mass % LSs added with IA led to an increase in the amount of bound water after 30 minutes of hydration, compared to the respective samples without LSs. This was explained by an increased amount of ettringite, which also is reflected in a higher surface area, as measured with BET (see Figure 8). For CX cement, the unexpected lack of any decrease in yield stress and the increase in viscosity at 30 minutes of hydration, as displayed in Figure 2 b, are therefore most likely due to the high amount of ettringite formed. A production of large amounts of ettringite was found to cause slump loss by, amongst others, Hanehara and Yamada [40]. The increase in amount of ettringite was larger for CX than for ANL cement. Accordingly, CX cement displayed a larger reduction in workability compared to ANL cement.

Moreover, the initial yield stress (without LSs) was remarkably higher for CX than for ANL cement paste. This is most likely due both to the higher content of $C_3A$ in CX cement and to the smaller particle size of the CX cement, leading to higher surface area available to interact with water and plasticizer, and thus higher reactivity.

### 4.3 Setting time

The setting retardation was calculated as the setting time measured with calorimetry, from which the setting time of the sample without LSs was subtracted. In Figure 9 a and b the setting retardation is related to the amount of total and free LSs, respectively.

It should be noted that it is unclear which of the different components of LSs cause the effects discussed in the following e.g. sugars or the lignosulphonate molecules. The LSs is considered as a whole. To distinguish the contributions of the different constituents further research is required. For DA, total LSs dosages higher than about 0.25 mass % led to a major setting retardation (see Figure 9a). For IA, a more gradual increase in setting time was measured as the LSs added increased. Both for IA and for DA, the setting retardation was higher for ANL than for CX cement.

The results shown in Figure 9b indicate correlations between the setting retardation and the amount of free LSs in the pore solution. For LSs dosages over about 0.25 mass %, any increase in free LSs corresponded to a large increase in setting retardation, especially for samples mixed with DA. Over this dosage, the samples mixed with DA also displayed a drop in yield stress, as discussed in paragraph 4.2 and showed in Figure 1 and in Figure 2. These results seem to agree with the conclusions of Yamada et al. [41], who stated a progressive increase in setting time with a higher concentration of free sulfonic and carboxylic groups in the aqueous phase.

At equal amount of free LSs in the pore solution, a higher setting retardation was measured for ANL cement than for CX cement. The setting retardation was higher for DA than for IA. This might be due to several reasons:

First, in a previous paper [32, 39], increasing LSs dosages added with IA were found to increase the amount of ettringite formed in cement paste. The increase as measured with TGA was larger for CX cement compared to ANL cement, and for IA compared to DA. An increased initial ettringite formation due to LSs addition with IA was also reported by Danner et al. [42]. In another paper, Danner et al. [43] found that Ca-LSs added with IA to a $C_3A$-gypsum system led to changes in the ettringite morphology, which appeared as wider, shorter and more rounded crystals. According to Zingg et al. [44], the smaller cubic ettringite crystals can be finely dispersed by the plasticizer, providing additional nucleation surface. In the present paper, the possible formation of a larger amount of smaller and more compact ettringite crystals could lead to the lower setting retardation measured for CX cement compared to ANL cement, and for IA compared to DA because of the additional nucleation surface.

As shown in Figure 4 and Figure 5, increasing LSs dosages led to larger retardation of the silicate peak compared to the aluminate one, causing the two peaks to merge in most samples with the higher LSs dosages analyzed. Similar observations were made in several studies [45-48], in which it was even observed that the aluminate peak could occur earlier than the silicate one upon high plasticizer dosages. This might lead to poisoning of the $C_3S$ hydration and uncontrolled delay of setting. This is a commonly known phenomenon leading to incompatibility issues between plasticizer and cement. In light of the results reported in the present article, the smaller retardation of the $C_3A$ peak compared to the $C_3S$ one, or even the occurrence of the aluminate peak before the silicate one, might be partially explained by the enhanced precipitation of ettringite within the first 30 minutes of hydration, which could lead to a faster consumption of sulfates, thus to an earlier sulfate depletion point.

Regarding the difference in setting retardation between the two cements, Pourchet et al. [49] found that the sulfate type used modified the early $C_3A$-$CaSO_4$ hydrates and their rate of formation. The substitution of gypsum with hemihydrate increased the rate of ettringite formation during the first five hours of hydration. The difference in sulfate type between ANL and CX cements (gypsum and hemihydrate for ANL cement, hemihydrate and anhydrite for CX cement) could then be one of the reasons why more ettringite was formed in CX cement than in ANL cement. Moreover, the higher

447 content in $C_3A$ of CX cement and its smaller particle size could allow a higher amount of $C_3A$ to enter
448 in contact with water, favouring the production of ettringite compared to ANL cement.

449 Finally, aluminum ions dissolved in the pore solution appeared to negatively impact the $C_3S$ hydration,
450 both by increasing its induction period [50, 51], and by reducing the extent of its hydration [52]. The
451 results from ICP-MS, displayed in Figure 6, showed that an increased concentration of Al was
452 measured in the pore solution of both cements solely when mixed with DA. The Al concentration was
453 higher for ANL than for CX cement. One of the hypothesized explanations for the retarding effect of
454 Al on $C_3S$ reaction is the substitution of some silicates by the Al ions with consequent formation of C-
455 A-S-H instead of C-S-H. Since the first C-A-S-H nuclei do not grow nor support hydrates nucleation
456 as C-S-H does, the $C_3S$ induction period is extended [53]. Another possible explanation was given by
457 Nicoleau et al. [54], who found that Al ions covalently bind to the silicates on the $C_3S$ surface,
458 strongly inhibiting $C_3S$ dissolution. The poisoning of $C_3S$ by Al ions, with consequent delay in $C_3S$
459 hydration, appears then to be a feasible explanation for the increased setting retardation measured for
460 DA compared to IA.

461 ## 5 CONCLUSIONS
462

463 The aim of this paper was to obtain a better understanding of the effects of calcium lignosulfonate
464 (LSs) on the rheology and setting time of Portland cement pastes. Two Portland cements mainly
465 differing in surface area and $C_3A$ content were used. The LSs was either added immediately with the
466 mixing water (IA), or delayed after 10 minutes of hydration (DA). The following conclusions were
467 drawn:

468 - The rheological behavior relates to the degree of LSs coverage of the available surface for
469 adsorption. A drop in yield stress and viscosity was measured for the cement pastes that
470 reached an adsorption plateau, as observed for DA. Samples which did not reach surface
471 saturation showed a more gradual improvement in workability, as observed for IA.

- An increased formation of ettringite, which was observed with elevated LSs dosages for IA, might lead to early hardening of the cement paste.
- The setting behavior appears to relate to the amount of free LSs in the pore solution.
- The difference in setting retardation between IA and DA might be related to the amount of ettringite formed in the system. Indeed:
    - The ettringite might supply additional surface area, which increase the amount of LSs consumed by monolayer adsorption. The consequent reduced amount of free LSs in the pore solution was reflected in a lower setting retardation.
    - Enhanced ettringite formation might supply additional nucleation surface, thus reducing the setting retardation when compared to a reference sample without LSs.
    - Increased ettringite precipitation could lead to a faster consumption of sulfates, thus to an earlier sulfate depletion.
    - Increased ettringite formation resulted in less Al dissolved in the pore solution and available to interact and retard the $C_3S$ hydration.

## 6 FUTURE RESEARCH

In a follow-up study, the effect of LSs on the amount and morphology of ettringite and other early cement hydrates produced both for IA and DA will be investigated. The effect of LSs on the hydrates formed in the hardened cement paste will also be considered for future research.

## 7 ACKNOWLEDGEMENTS

The authors wish to acknowledge the Norwegian Research Council (NFR 225358/O30) and Borregaard AS, Norway, for financing this research work. Gwenn Le Saoût and Nathalie Azéma, Ecole des Mines d'Alès, France, are also acknowledged for the helpful discussions. Irene Bragstad, SINTEF, Norway, is acknowledged for performing the BET measurements. Syverin Lierhagen, NTNU, Norway, is acknowledged for performing the ICP-MS analysis.

# 8 REFERENCES


[1] Y. Zhang, M. Collepardi, L. Coppola, W. Guan, P. Zaffaroni, Optimization of the High-Strength Superplasticized Concrete for the 3-Gorges Dam in China, Industria Italiana del Cemento 783 (2003) 58-69.

[2] L. Coppola, T. Cerulli, D. Salvioni, Sustainable development and durability of self-compacting concretes, in: V.M. Malhotra (Ed.) 8th CANMET/ACI international conference on fly ash, silica fume, slag, and natural pozzolans in concrete, 2004, pp. 29-50.

[3] Y.F. Houst, P. Bowen, F. Perche, A. Kauppi, P. Borget, L. Galmiche, J.-F. Le Meins, F. Lafuma, R.J. Flatt, I. Schober, P.F.G. Banfill, D.S. Swift, B.O. Myrvold, B.G. Petersen, K. Reknes, Design and function of novel superplasticizers for more durable high performance concrete (superplast project), Cement and Concrete Research 38 (2008) 1197-1209.

[4] H. Vikan, Rheology and reactivity of cementitious binders with plasticizers, Department of Materials Science and Engineering, NTNU Trondheim, 2005.

[5] M. Bishop, S.G. Bott, A.R. Barron, A New Mechanism for Cement Hydration Inhibition: Solid-State Chemistry of Calcium Nitrilotris(methylene)triphosphonate, Chemistry of Materials 15(16) (2003) 3074-3088.

[6] J. Cheung, A. Jeknavorian, L. Roberts, D. Silva, Impact of admixtures on the hydration kinetics of Portland cement, Cement and Concrete Research 41(12) (2011) 1289-1309.

[7] D. Marchon, R.J. Flatt, 12 - Impact of chemical admixtures on cement hydration, Science and Technology of Concrete Admixtures, Woodhead Publishing2016, pp. 279-304.

[8] D. Jansen, J. Neubauer, F. Goetz-Neunhoeffer, R. Haerzschel, W.D. Hergeth, Change in reaction kinetics of a Portland cement caused by a superplasticizer — Calculation of heat flow curves from XRD data, Cement and Concrete Research 42(2) (2012) 327-332.

[9] N.L. Thomas, J.D. Birchall, The retarding action of sugars on cement hydration, Cement and Concrete Research 13(6) (1983) 830-842.

[10] J.F. Young, A review of the mechanisms of set-retardation in portland cement pastes containing organic admixtures, Cement and Concrete Research 2(4) (1972) 415-433.

[11] M. Collepardi, The influence of admixtures on concrete rheological properties, Il cemento1982.

[12] V.S. Ramachandran, R.F. Feldman, Adsorption of calcium lignosulfonate on tricalcium aluminate and its hydrates in a non-aqueous medium, Cement technology1971, pp. 121-129.

[13] V. Lorprayoon, D.R. Rossington, Early hydration of cement constituents with organic admixtures, Cement and Concrete Research 11(2) (1981) 267-277.

[14] K. Reknes, J. Gustafsson, Effect of modifications of lignosulfonate on adsorption on cement and fresh concrete properties, 7th International Conference on Superplasticizers and Other Chemical Admixtures in Concrete, 2000, pp. 127-142.

[15] V.S. Ramachandran, Interaction of calcium lignosulfonate with tricalcium silicate, hydrated tricalcium silicate, and calcium hydroxide, Cement and Concrete Research 2(2) (1972) 179-194.

[16] S. Monosi, G. Moriconi, M. Collepardi, Combined effect of lignosulfonate and carbonate on pure portland clinker compounds hydration. III. Hydration of tricalcium silicate alone and in the presence of tricalcium aluminate, Cement and Concrete Research 12(4) (1982) 425-435.

[17] M. Collepardi, A. Marcialis, V. Solinas, The influence of calcium lignosulfonate on the hydration of cements, Il cemento1973.

[18] V.S. Ramachandran, Interaction of admixtures in the cement-water system, Application of admixtures in concrete, CRC Press1994.

[19] J.F. Young, Hydration of tricalcium aluminate with lignosulphonate additives, Magazine of Concrete Research 14(42) (1962) 137-142.

[20] S. Monosi, G. Moriconi, M. Pauri, M. Collepardi, Influence of lignosulphonate, glucose and gluconate on the C3A hydration, Cement and Concrete Research 13(4) (1983) 568-574.

[21] R.J. Flatt, Y.F. Houst, A simplified view on chemical effects perturbing the action of superplasticizers, Cement and Concrete Research 31 (2001) 1169-1176.

549 [22] M. Collepardi, L. Coppola, T. Cerulli, G. Ferrari, C. Pistolesi, P. Zaffaroni, F. Quek, Zero slump-
550 loss superplasticized concrete, in: C.T. Tam (Ed.) 18th Conference on Our world in concrete &
551 structures, Singapore, 1993.
552 [23] M. Collepardi, L. Coppola, T. Cerulli, G. Ferrari, C. Pistolesi, P. Zaffaroni, G. Desroches, A.
553 Drapeau, Acrylic based superplasticizers, 4th CANMET/ACI international conference on
554 superplasticizers and other chemical admixtures in concrete, Montreal, Canada, 1994, pp. 1-18.
555 [24] H. Uchikawa, S. Hanehara, T. Shirasaka, D. Sawaki, Effect of admixture on hydration of cement,
556 adsorptive behaviour of admixture and fluidity and setting of fresh cement paste, Cement and
557 Concrete Research 22(6) (1992) 1115-1129.
558 [25] G. Chiocchio, A.E. Paolini, Optimum time for adding superplasticizer to Portland cement pastes,
559 Cement and Concrete Research 15(5) (1985) 901-908.
560 [26] I. Aiad, S. Abd El-Aleem, H. El-Didamony, Effect of delaying addition of some concrete
561 admixtures on the rheological properties of cement pastes, Cement and Concrete Research 32(11)
562 (2002) 1839-1843.
563 [27] J. Hot, Influence des polymères de type superplastifiants et agents entraineurs d'air sur la
564 viscosité macroscopique des matériaux cimentaires, Université Paris-Est, Paris, 2013.
565 [28] K.-C. Hsu, J.-J. Chiu, S.-D. Chen, Y.-C. Tseng, Effect of addition time of a superplasticizer on
566 cement adsorption and on concrete workability, Cement and Concrete Composites 21(5–6) (1999)
567 425-430.
568 [29] I. Aiad, Influence of time addition of superplasticizers on the rheological properties of fresh
569 cement pastes, Cement and Concrete Research 33 (2003) 1229-1234.
570 [30] N. Roussel, Rheology of fresh concrete: from measurements to predictions of casting processes,
571 Materials and Structures 40(10) (2007) 1001-1012.
572 [31] J. Hot, H. Bessaies-Bey, C. Brumaud, M. Duc, C. Castella, N. Roussel, Adsorbing polymers and
573 viscosity of cement pastes, Cement and Concrete Research 63 (2014) 12-19.
574 [32] A. Colombo, M. Geiker, H. Justnes, R.A. Lauten, K. De Weerdt, On the mechanisms of
575 consumption of calcium lignosulfonate by cement paste, Cement and Concrete Research (2016, In
576 review).
577 [33] G. Le Saoût, V. Kocaba, K. Scrivener, Application of the Rietveld method to the analysis of
578 anhydrous cement, Cement and Concrete Research 41(2) (2011) 133-148.
579 [34] R.G. Gilbert, M. Hess, A.D. Jenkins, R.G. Jones, P. Kratochvil, R.F.T. Stepto, Dispesity in
580 polymer science, Pure applied chemistry 81(2) (2009) 351-353.
581 [35] H. Vikan, H. Justnes, F. Winnefeld, R. Figi, Correlating cement characteristics with rheology of
582 paste, Cement and Concrete Research 37(11) (2007) 1502-1511.
583 [36] F. Perche, Adsorption de Polycarboxylates et de Lignosulfonates sur Poudre modele et Ciments,
584 École Polytechnique Federale de Lausanne, 2004.
585 [37] K.R. Ratinac, O.C. Standard, P.J. Bryant, Lignosulfonate adsorption and stabilization of lead
586 zirconate titanate in aqueous suspension, Journal of Colloid and Interface Science 273 (2004) 442-454.
587 [38] P.C. Hiemenz, R. Rajagopalan, Principles of colloid and surface chemistry, Taylor & Francis
588 Group1997.
589 [39] A. Colombo, M. Geiker, H. Justnes, R.A. Lauten, K. De Weerdt, On the mechanisms of
590 consumption of calcium lignosulfonate by cement paste, Cement and Concrete Research (In review).
591 [40] S. Hanehara, K. Yamada, Interaction between cement and chemical admixture from the point of
592 cement hydration, absorption behaviour of admixture, and paste rheology, Cement and Concrete
593 Research 29(8) (1999) 1159-1165.
594 [41] K. Yamada, T. Takahashi, S. Hanehara, M. Matsuhisa, Effects of the chemical structure on the
595 properties of polycarboxylate-type superplasticizer, Cement and Concrete Research 30(2) (2000) 197-
596 207.
597 [42] T. Danner, H. Justnes, M. Geiker, R.A. Lauten, Phase changes during the early hydration of
598 Portland cement with Ca-lignosulfonates, Cement and Concrete Research 69(0) (2015) 50-60.
599 [43] T. Danner, H. Justnes, M. Geiker, R.A. Lauten, Early hydration of C3A–gypsum pastes with Ca-
600 and Na-lignosulfonate, Cement and Concrete Research 79 (2016) 333-343.
601 [44] A. Zingg, F. Winnefeld, L. Holzer, J. Pakush, S. Becker, L. Gauckler, Adsorption of
602 polyelectrolytes and its influence on the rheology, zeta potential, and microstructure of various cement
603 and hydrate phases, Journal of Colloid and Interface Science 323 (2008) 301-312.

[45] P. Sandberg, L.R. Roberts, Studies of cement-admixture interactions related to use of chemical admixtures, 7th CANMET/ACI International Conference on Superplasticizers and other chemical Admixtures in concrete, 2003, pp. 529-542.
[46] D. Marchon, M. Jachiet, R.J. Flatt, P. Juilland, Impact of polycarboxylate superplasticizers on polyphased clinker hydration, 34th cement and concrete science conference, Sheffield, UK, 2014, pp. 79-82.
[47] L.H. Tuthill, R.F. Adams, S.N. Bailey, R.W. Smith, A case of abnormally slow hardening concrete for tunnel lining, ACI Journal 57(3) (1961) 1091-1109.
[48] L.R. Roberts, P.C. Taylor, Understanding cement-SCM-admixture interaction issues, Concrete international (2007) 33-41.
[49] S. Pourchet, L. Regnaud, J.P. Perez, A. Nonat, Early C3A hydration in the presence of different kinds of calcium sulfate, Cement and Concrete Research 39(11) (2009) 989-996.
[50] I. Odler, J. Schüppstuhl, Early hydration of tricalcium silicate III. Control of the induction period, Cement and Concrete Research 11(5–6) (1981) 765-774.
[51] G.L. Valenti, V. Sabatelli, B. Marchese, Hydration kinetics of tricalcium silicate solid solutions at early ages, Cement and Concrete Research 8(1) (1978) 61-72.
[52] A. Quennoz, Hydration of C3A with Calcium Sulfate Alone and in the Presence of Calcium Silicate, EPFL, 2011.
[53] F. Begarin, S. Garrault, A. Nonat, L. Nicoleau, Hydration of alite containing alumimium, 29 th Cement and Concrete Science Congress, Leeds, 2009, pp. 9-12.
[54] L. Nicoleau, E. Schreiner, A. Nonat, Ion-specific effects influencing the dissolution of tricalcium silicate, Cement and Concrete Research 59 (2014) 118-138.

## Notation

| | |
|---|---|
| ANL | Anlegg cement (CEM I 52.5 N) |
| CX | Cemex cement (CEM I 52.5 R) |
| DA | delayed addition of plasticizer (10 min) |
| IA | immediate addition of plasticizer |
| LSs | softwood low-sugar Ca-lignosulfonate |
| OPC | ordinary Portland cement |
| w/b | water-binder ratio |
| $\dot{\gamma}$ | shear rate |
| $\tau$ | shear stress |
| $\mu$ | viscosity |

639 -COOH carboxyl group

640 φ-OH phenolic OH-group

641

642 List of tables

643


656

657 List of figures

658

Table 1 – *Main phases in cement ANL and CX from XRD-Rietveld analysis [a]: results obtained with TGA analysis*

| **Phase composition (mass %)** | **ANL** | **CX** |
|---|---|---|
| **Alite** | 60.5 | 54.3 |
| **Belite** | 14.2 | 18.8 |
| **Aluminate cubic** | 1.3 | 4.7 |
| **Aluminate orthorhombic** | 0.9 | 2.4 |
| **Ferrite** | 14.0 | 6.5 |
| **Periclase** | 0.4 | 1.1 |
| **Quartz** | 0.3 | - |
| **Calcite** | 3.2/ 3.8 [a] | 3.6/ 3.7 [a] |
| **Portlandite** | 1.1/ 1.4 [a] | 2.6/ 2.5 [a] |
| **Anhydrite** | - | 2.1 |
| **Hemihydrate** | 2.6 | 1.8 |
| **Gypsum** | 1.0 | - |
| **Arcanite** | | 0.6 |
| **Aphthitalite** | 0.4 | 0.7 |

| | | |
|---|---|---|
| **Thenardite** | - | 0.8 |

687

688

689 Table 2 – *Chemical composition of the cements given by the producers*

| **Chemical compound (mass %)** | **ANL** | **CX** |
|---|---|---|
| **CaO** | 62.7 | 64.0 |
| **$SiO_2$** | 20.6 | 20.0 |
| **$Al_2O_3$** | 4.4 | 4.6 |
| **$Fe_2O_3$** | 3.5 | 2.6 |
| **$SO_3$** | 3.3 | 3.6 |
| **MgO** | 1.6 | 2.4 |
| **$K_2O$** | 0.4 | 1.0 |
| **$Na_2O$** | 0.3 | 0.2 |
| **$TiO_2$** | 0.2 | 0.2 |
| **$P_2O_5$** | 0.2 | 0.2 |
| **LOI (%) 1000 °C** | 1.6 | 1.7 |
| **Sum** | 97.2 | 98.9 |

690

691

692 Table 3 - *Physical properties of ANL and CX cements*

| | **ANL** | **CX** |
|---|---|---|
| **Surface area (BET) ($m^2/kg$)** | 890 | 1330 |
| **Blaine surface ($m^2/kg$)** | 360 | 540 |
| **Density ($g/cm^3$)** | 3.1 | 3.1 |
| **$d_{10}$ (µm)** | 2.0 | 2.0 |
| **$d_{50}$ (µm)** | 12.0 | 10.0 |
| **$d_{90}$ (µm)** | 34.0 | 26.0 |

693

694 Table 4 - *Chemical and physical properties of LSs*

| | | |
|---|---|---|
| **Mw** | g/mol | 29000 |
| **Mn** | g/mol | 2100 |
| **Organic S** ($\propto SO_3$) | mass % | 4.6 |
| **$SO_4^{2-}$** | mass % | 0.9 |
| **$Ca^{2+}$** | mass % | 4.6 |
| **$Na^{+}$** | mass % | 0.9 |
| **-COOH** | mass % | 7.1 |
| **φ-OH** | mass % | 1.4 |
| **Total sugar** | mass % | 8.3 |

695

696

697 Table 5 – *Sequence for rheology measurements*

| | | **Duration** (s) | **Cumulative duration** (min) |
|---|---|---|---|
| 1 | Stir up at $\dot{\gamma}$ = 60 1/s | 30 | 0.5 |
| 2 | Rest | 30 | 1.0 |
| 3 | Flow curve up, linear sweep $\dot{\gamma}$ from 0 to 60 1/s in 20 steps lasting 5 sec. each | 100 | 2.7 |
| 4 | Flow curve down, linear sweep $\dot{\gamma}$ from 60 to 0 1/s in 20 steps lasting 5 sec. each | 100 | 4.3 |
| 5 | Rest | 340 | 10.0 |
| 6 | Stir up at $\dot{\gamma}$ = 60 1/s | 30 | 10.5 |
| 7 | Rest | 30 | 11.0 |
| 8 | Flow curve up, linear sweep $\dot{\gamma}$ from 0 to 60 1/s in 20 steps lasting 5 sec. each | 100 | 12.7 |
| 9 | Flow curve down, linear sweep $\dot{\gamma}$ from 60 to 0 1/s in 20 steps lasting 5 sec. each | 100 | 14.3 |
| 10 | Rest | 340 | 20.0 |
| 11 | Stir up at $\dot{\gamma}$ = 60 1/s | 30 | 20.5 |
| 12 | rest | 30 | 21.0 |
| 13 | Flow curve up, linear sweep $\dot{\gamma}$ from 0 to 60 1/s in 20 steps lasting 5 sec. each | 100 | 22.7 |
| 14 | Flow curve down, linear sweep $\dot{\gamma}$ from 60 to 0 1/s in 20 steps lasting 5 sec. each | 100 | 24.3 |

698

699

700 Table 6 – *Analysed samples to obtain adsorption isotherms*

| Material | LSs addition procedure | LSs dosage (mass % binder) |
|---|---|---|
| **ANL cement** | IA | 0.1; 0.2; 0.4; 0.6; 0.8; 1.2; 1.5 |
| | DA | 0.05; 0.1; 0.25; 0.4; 0.8; 1.2; 1.5 |
| **CX cement** | IA | 0.1; 0.2; 0.4; 0.6; 0.8; 1.0 |
| | DA | 0.05; 0.1; 0.2; 0.4; 0.8; 1.2; 1.5 |

701

702

703 Table 7 – *The dynamic yield stress and plastic viscosity of the reference mixes ANL and CX without*

704 *LSs addition, 10 and 30 min after water addition*

| | | ANL | CX |
|---|---|---|---|
| **Yield stress (Pa)** | 10 min | 67 | 121 |
| | 30 min | 81 | 145 |
| **Viscosity (Pa.s)** | 10 min | 0.58 | 1.7 |
| | 30 min | 0.75 | 2.2 |

705

706

707

Table 8 – *Elemental concentration of Al, Fe, Ca, Si, and S in ANL and CX cements with 0, 0.8 or 1.5 mass % LSs after 30 minutes hydration, and in two LSs solutions (mmol/L): the 2.0 and 3.7 % LSs solutions were used for the cement samples with 0.8 and 1.5 mass % LSs respectively*

| **Sample** | **LSs dosage** | **Al** | **Ca** | **Fe** | **S** | **Si** |
|---|---|---|---|---|---|---|
| | Mass % binder | | | Mass % | | |
| **ANL IA** | 0 | 0.05 | 236 | 0.03 | 767 | 0.86 |
| | 0.8 | 0.07 | 260 | 0.09 | 963 | 1.1 |
| | 1.5 | 0.15 | 445 | 0.69 | 1390 | 1.2 |
| **ANL DA** | 0.8 | 11.2 | 375 | 5.5 | 1003 | 8.5 |
| | 1.5 | 35.7 | 523 | 14.3 | 715 | 26.0 |
| **CX IA** | 0 | 0.05 | 239 | 0.02 | 1759 | 0.90 |
| | 0.8 | 0.06 | 103 | 0.2 | 1691 | 3.0 |
| | 1.5 | 0.11 | 53.7 | 1.1 | 1414 | 3.6 |
| **CX DA** | 0.8 | 0.96 | 282 | 1.1 | 1762 | 2.3 |
| | 1.5 | 7.9 | 499 | 4.5 | 1929 | 5.6 |
| **2.0 % LSs sol.** | | 0.18 | 183 | 0.19 | 370 | 3.1 |
| **3.7 % LSs sol.** | | 0.26 | 324 | 0.31 | 659 | 2.7 |

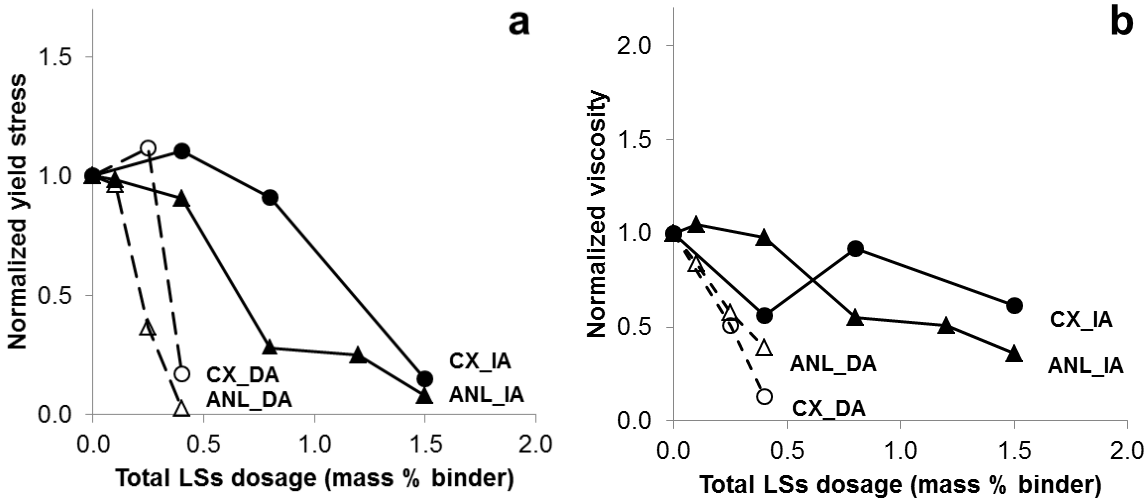


713

714 Figure 1 – *a) Normalized yield stress and b) normalized viscosity vs. total LSs (mass % binder) of ANL*

715 *and CX cements mixed with IA or DA of LSs at 10 min of hydration (12 min of hydration for samples*

716 *prepared with DA)*

717

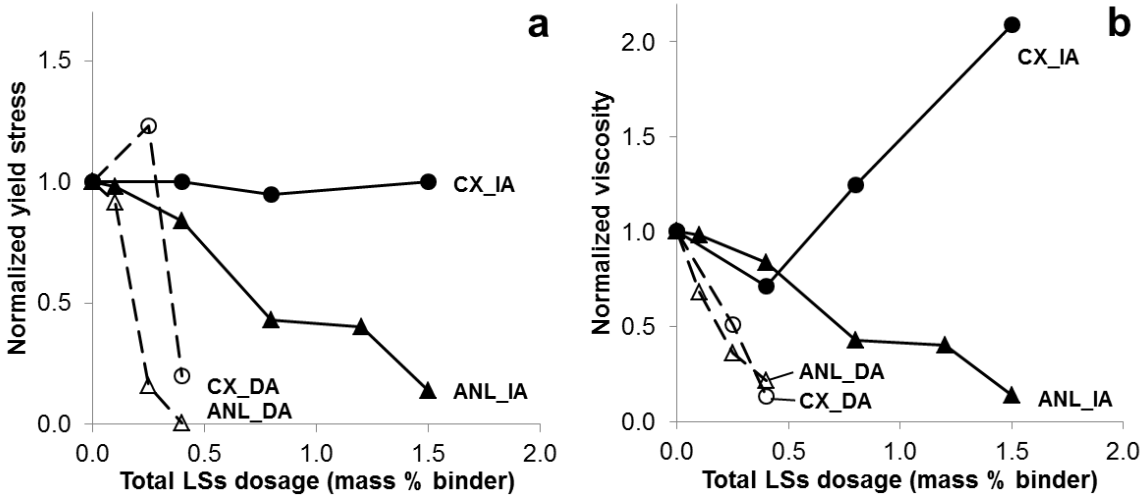


718

719 Figure 2– *a) Normalized yield stress and b) normalized viscosity vs. total LSs (mass % binder) of ANL*

720 *and CX cements mixed with IA or DA of LSs at 30 min of hydration*

721

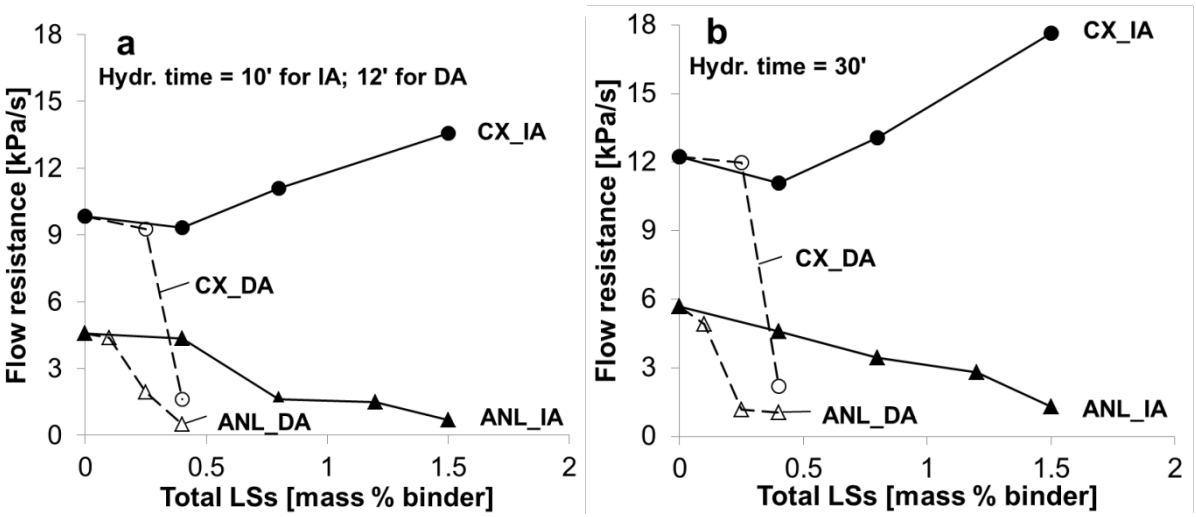


722

723 Figure 3 - *Flow resistance at 10 min. of hydration (12 min of hydration for samples prepared with DA)*
724 *in fig. a and at 30 min. of hydration in fig. b vs. total LSs(mass % binder) of ANL and CX cements with*
725 *IA or DA of LSs*

726

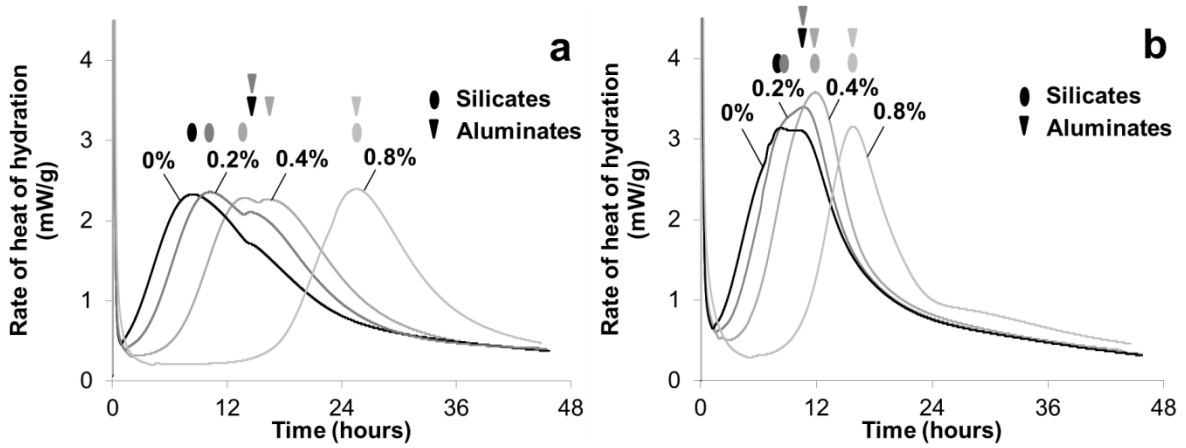


727

728 Figure 4 – *Rate of heat of hydration in time for a) ANL and b) CX cement pastes with increasing*
729 *dosage of LSs mixed with IA (0, 0.2, 0.4, 0.8 mass % LSs). The silicates and aluminates peaks are*
730 *marked with different symbols in corresponding colour of the respective calorimetric curve.*

731

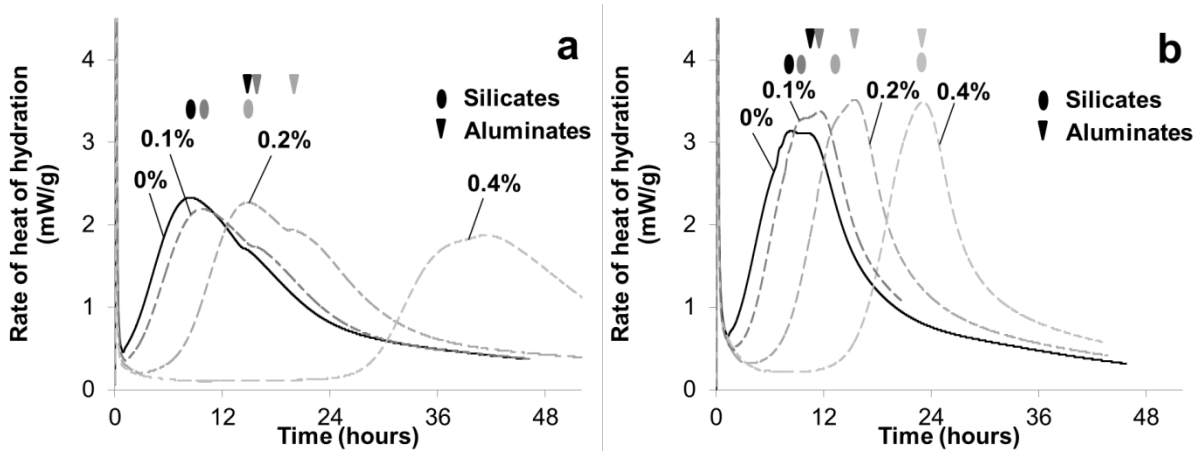


732

733 Figure 5 - *Rate of heat of hydration vs. time for a) ANL and b) CX cement pastes with increasing*
734 *dosage of LSs mixed with DA (0, 0.1, 0.2, 0.4 mass % LSs). The silicates and aluminates peaks are*
735 *marked with different symbols in corresponding color of the respective calorimetric curve.*

736

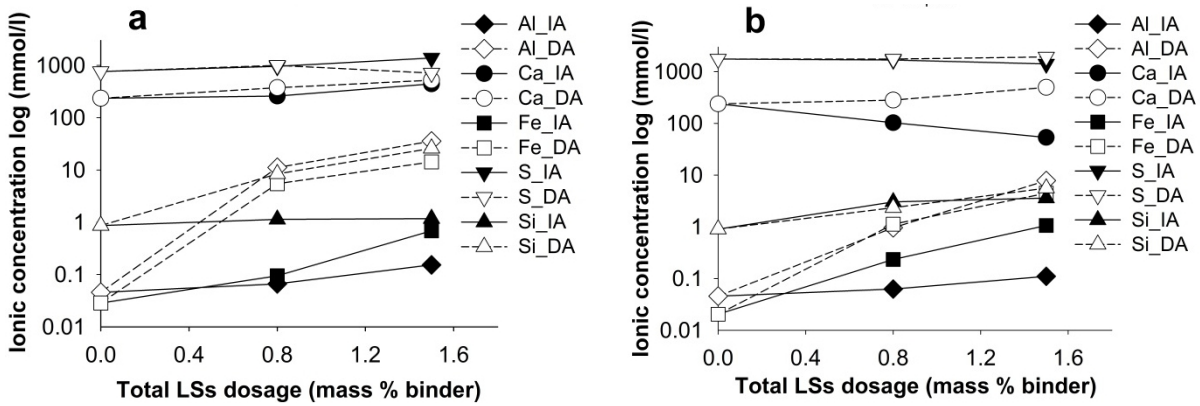


737

738 Figure 6 – *Concentration of Al, Fe, Ca, Si, and S ions in the pore solution (mmol/L) expressed in*
739 *logarithmic scale vs. total LSs added (mass % binder) to a) ANL and b) CX cement pastes at 30 min of*
740 *hydration both for IA and DA*

741

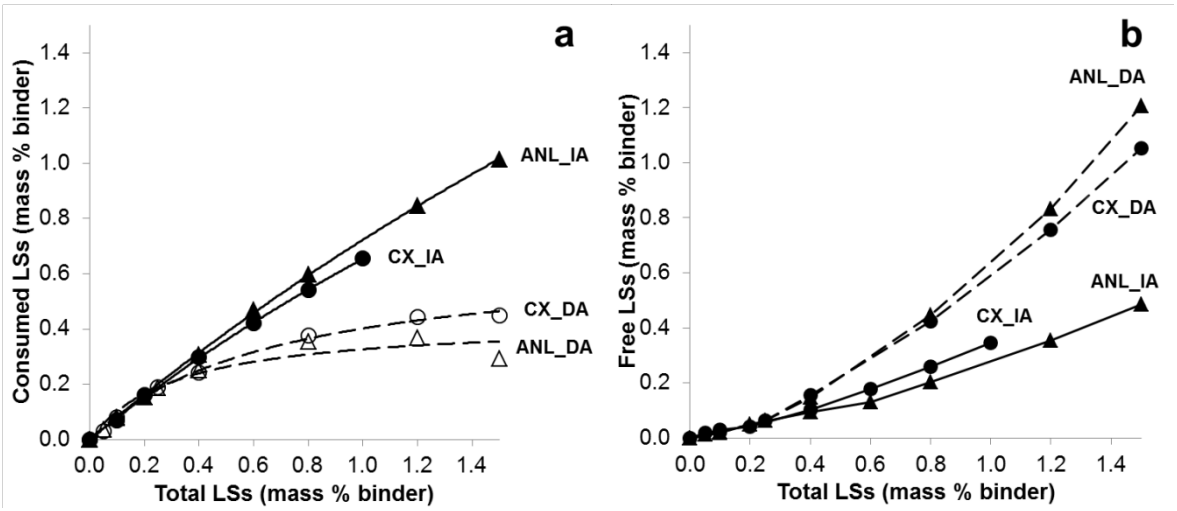


742

743 Figure 7 - *Amount of a) consumed LSs and of b) free LSs at 30 min of hydration vs. amount of LSs*
744 *added to ANL and CX cements for IA and DA, after [32]. The results are calculated per mass % of*
745 *binder*

746

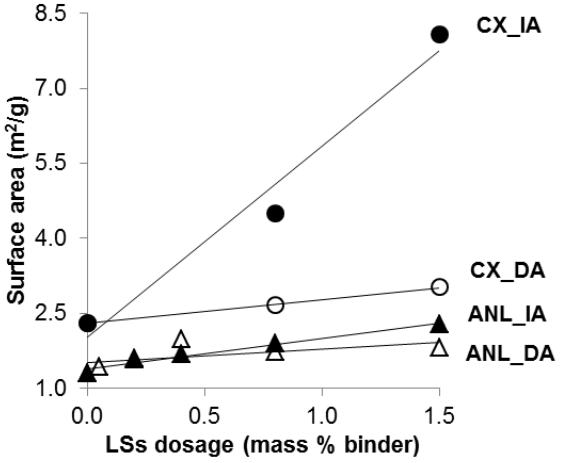


747

748 Figure 8 - *Surface area of ANL and CX cement particles hydrated for 30 min vs. total dosage of LSs*
749 *added (mass % binder) both for IA and DA, after [32]*

750

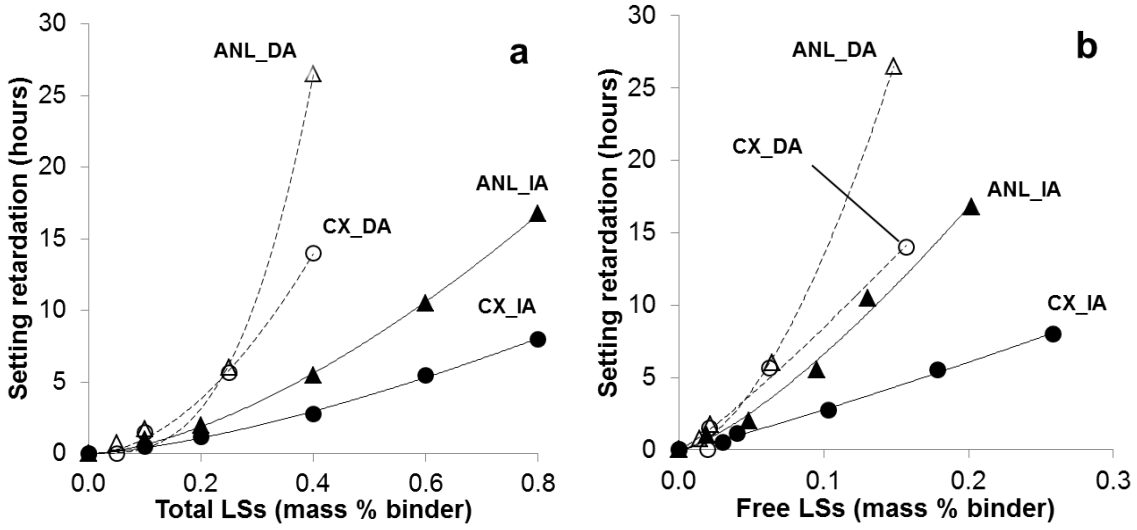


751

752 Figure 9 – *Setting time retardation vs. amount of a) total LSs and b) free LSs for ANL and CX cement*

753 *pastes containing increasing dosage of LSs both for IA and DA. NB. The figures' scales are different.*